RSC Advances

ROYAL SOCIETY OF CHEMISTRY

www.rsc.org/advances

ARTICLE TYPE www.rsc.org/xxxxxx | XXXXXXXX

Solvent-controlled Structural Diversity Observed in Three Cu(II) MOFs with 2,2'-dinitro-biphenyl-4,4'-dicarboxylate Ligand: Synthesis, Structures and Magnetism

Na Zhang,[a] Jian-Yong Zhang,*[a] Qin-Xiang Jia,[b] Wei Deng,[a] and En-Qing Gao*[c]

Three extended three-dimensional Cu^{II}-based metal-organic frameworks (MOFs) have been separated successfully from reactions of 2,2'-dinitro-biphenyl-4,4'-dicarboxylate (H_2dnpdc) ligand and $Cu(NO_3)_2$ under controllable solvothermal conditions. The resulting structures of the MOFs are highly dependent on the solvent used during the synthesis. Compound **1**, $[Cu(dnpdc)(H_2O)]_n \cdot (DMA)_4(H_2O)_2$, is a two-fold interpenetrated three-dimensional framework with *NbO* topology based on binuclear $[Cu_2(O_2C)_4]$ "paddle-wheel" secondary building unit; In compound **2**, $[Cu_9(dnpdc)_6(OH)_6(H_2O)_2]_n \cdot \{(DMF)_8(EtOH)_3(H_2O)_{12}\}_n$, the complicated one-dimensional $[Cu(OH)(OCO)]_n$ chain are cross-linked into three-dimensional framework by the $dnpdc^{2-}$ ligands; Compound **3**, $\{Cu_4(dnpdc)_3(OH)_2(py)_4\}_n$, displays three-dimensional net with *pcu* topology based on 6-connected $[Cu(\mu_3\text{-}OH)_2(OCO)_4]$ tetracopper cluster. Magnetically, compound **2** exhibits homo-spin topological ferrimagnetic behavior. Compound **3** features antiferromagnetic interactions mediated by μ_3-OH and *syn-syn*-OCO heterobridges between the Cu^{II} ions.

Introduction

In the past 20 years, porous metal-organic Frameworks (MOFs) or coordination polymers (CPs) based upon the self-assembly of metal ions / clusters and polydentate bridging ligands have spawned tremendous attention of supramolecular and material chemists all over the world, not only for their fascinating diverse structures but also their useful properties relevant to applications such as gas adsorption / separation, heterogeneous catalysis, drug delivery, luminescence, chemical sensing and magnetism[1-7]. In general, practical applications of MOFs are directly related to their structural features. However, how to rationally realize the preferred structures with specific functionalities still remain a still challenge because that the self-assembly of MOFs is influenced by many factors, such as the metal-to-ligand molar ratio, the pH value, reaction temperature, even the reaction solvent, and subtle changes of the synthesis conditions can lead to the one or the other topology structures of the final compounds[8]. In our previous work, we have shown the metal-to-ligand molar ratio, pH value and temperature effects on the final structures of a series of 2,2'-dinitro-biphenyl-4,4'-dicarboxylic acid (H_2dnpdc)-based MOFs[9]. In addition to the temperature and the pH value, the solvent used is also an important factor because its structure and chemical properties can influence the rate of crystal growth and even the final structures, and several examples of solvent-dependent MOFs have been reported to date[10]. As an extension and deepening of our former research on the H_2dnpdc ligand, we here reported three solvent-dependent Cu(II) compounds ligands exhibiting solvent-dependent structural varieties.

On the other hand, the study of magnetic metal-organic frameworks (MMOFs) have attracted much attention, since such materials can help in understanding magneto-structural correlations and some fundamental phenomena of magnetism, and may have potential applications[11,12]. The carboxylate ligands have been widely studied in this field for its versatilities in bridging metal ions and in inducing magnetic exchange between metal ions[13]. Polynuclear and polymeric Cu^{II} coordination compounds with carboxylate ligands have attracted much attention for decades[14], an elegant example is the Cu^{II} benzene-1,3,5-tricarboxylate (HKUST-1), based on the well-known dinuclear "paddle-wheel" $[Cu_2(O_2C)_4]$ secondary building units (SBUs), which has been subject to many magnetostructural studies[15]. The structural diversity of Cu^{II}-carboxylate systems is much enhanced by the incorporation of various co-ligands, such as hydroxo, alkoxo and azido, which can also mediate magnetic coupling effectively and are both capable of promoting ferromagnetic and antiferromagnetic interactions by adopting appropriate bridging mode and bridging angles[16-18]. We have been interested in aromatic dicarboxylate ligands, including the rigid 2,2'-dinitro-biphenyl-4,4'-dicarboxylic acid (H_2dnpdc). During the study, we have obtained some MOFs in which paramagnetic centres are aggregated by some short bridges, which are interesting for magnetic studies[12, 19]. Here, we present the synthesis, structures and magnetic properties of three Cu^{II}-based MOFs obtained from the reaction of $Cu(NO_3)_2$ with the H_2dnpdc ligand in different mixed solvent. Their formulas are $[Cu(dnpdc)(H_2O)]_n \cdot (DMA)_4(H_2O)_2$ (**1**), $[Cu_9(dnpdc)_6(OH)_6(H_2O)_2]_n \cdot \{(DMF)_8(EtOH)_3(H_2O)_{12}\}_n$ (**2**) and $\{Cu_4(dnpdc)_3(OH)_2(py)_4\}_n$ (**3**). The resulting structures of MOFs show highly dependence on the solvent used during the synthesis.

Experimental

Materials and physical measurements

The reagents were obtained from commercial sources and used without further purification. The ligand 2,2'-dinitro-biphenyl-4,4'-dicarboxylic acid (H_2dnpdc) was prepared according to the literature[20].

FT-IR spectra were recorded in the range 500 - 4000 cm^{-1}

on a Nicolet NEXUS 670 spectrophotometer using KBr pellets. Elemental analyses (C, H, and N) were performed on a Perkin-Elmer 2400 CHN elemental analyzer. Thermogravimetric analyses (TGA) were carried out on a Mettler Toledo TGA/SDTA851 instrument under flowing air at a heating rate of 5 °C/min. The powder X-ray diffraction (PXRD) was recorded on X'pert PRO diffractometer at 35 kV, 25mA for a Cu-target tube and a graphite monochromator. Temperature- and field-dependent magnetic measurements were carried out on a Quantum Design SQUID MPMS-5 magnetometer. Diamagnetic corrections were made with Pascal's constants.

Synthesis

$[Cu(dnpdc)(H_2O)]_n \cdot (DMA)_4(H_2O)_2$ (1). H_2dnpdc (0.075 mmol, 0.025 g) and $Cu(NO_3)_2$ (0.1 mmol, 0.024 g) were dissolved in DMA(N,N'-Dimethylacetamide)-EtOH-H_2O (5mL, v/v/v=3/1/1) mixture with 0.2mL ethyl glycol (EG) under stirring for 40 min at room temperature. The resulting mixture was then sealed in a capped vial and heated at 85 °C for 24 hours. After cooling to room temperature slowly, blue prism-shaped crystals of **1** were collected (yield: 76%). Elemental analysis calc. for ($C_{30}H_{48}N_6O_{15}Cu$, M =796.29): C, 45.25; H, 6.08; N, 10.55. Found: C, 45.09; H, 6.01; N, 10.12 %. IR (KBr, cm^{-1}): 3431br, 3092w, 2939w, 1693s, 1614s, 1529s, 1483m, 1406s, 1353vs, 1326m, 1300m, 1268m, 1147w, 1080m, 928m, 901w, 828w, 785m, 723m.

$[Cu_9(dnpdc)_6(OH)_6(H_2O)_2]_n \cdot \{(DMF)_8(EtOH)_3(H_2O)_{12}\}_n$ (2). The similar synthetic procedure of **1** was performed with DMF((N,N'-Dimethylformamide, 3mL) instead of DMA to generate pale-green crystals of compound **2** (yield: 62%). Elemental analysis calc. for ($C_{114}H_{144}N_{20}O_{79}Cu_9$, M =3630.4): C, 37.72; H, 4.00; N, 7.72. Found: C, 37.69; H, 3.97; N, 7.43 %. IR (KBr, cm^{-1}): 3080w, 2931w, 2872w, 1655s, 1614s, 1593s, 1533s, 1481m, 1406s, 1348s, 1256m, 1167w, 1134m, 1195m, 1063w, 1005m, 922m, 855w, 829m, 783m, 725m, 665m, 625w.

$\{Cu_4(dnpdc)_3(OH)_2(py)_4\}_n$ (3). H_2dnpdc (0.05 mmol, 0.016 g), $Cu(NO_3)_2$ (0.05 mmol, 0.012 g) was dissolved in DMF-EtOH-H_2O (4mL, v/v/v=1.5/1.5/1) under stirring at room temperature for 30 min, and then 1.0 mmol pyridine (0.079 g) and 0.2mL EG were added and allowed to stir for 1h more. The resulting mixture was then heated in a 23 mL Teflon-lined autoclave at 85 °C for 24h. After cooling to room temperature slowly, deep-blue block crystals of **3** were obtained (yield: 54%). Elemental analysis calc. for ($C_{62}H_{40}N_{10}O_{26}Cu_4$, M =1595.20): C, 46.68; H, 2.53; N, 8.78%. Found: C, 46.49; H, 3.04; N, 9.14 %. IR (KBr, cm^{-1}): 3083w, 2931w, 1653m, 1611vs, 1531vs,1484m, 1449m, 1385s, 1348s, 1253w, 1219w, 1131w, 1092w, 1009w, 913w, 863w, 826s, 787m, 762m, 723m, 699m.

Crystal structure analysis

Diffraction intensity data were collected at 153 K on a Bruker APEX II diffractometer equipped with a CCD area detector and graphite-monochromated Mo Kα radiation (λ = 0.71073 Å). Empirical absorption corrections were applied using the SADABS program[21]. The structures were solved by the direct method and refined by the full-matrix least-squares method on F^2, with all non-hydrogen atoms refined with anisotropic thermal parameters[22]. All the hydrogen atoms attached to carbon atoms were placed in calculated positions and refined using the riding model, and the water hydrogen atoms were located from the difference maps. The best diffraction data set after several attempts are still of limited quality. In compound **1** and **2**, the final structures have a large volume fraction of voids [67.8% and 46.1% for **1** and **2**, respectively] containing a number of residual electron density peaks, which may be attributed to disordered solvent molecules and could not be crystallographically defined satisfactorily. The SQUEEZE routine within the *PLATON* software package was applied to subtract the solvent contribution[23]. According to crystallographic data combined with elemental and thermogravimetric analyses, the solvent molecules were proposed to be DMA and H_2O molecules for **1** and DMF, EtOH, H_2O for **2**, respectively. Selected crystallographic data are summarized in Table 1.

CCDC reference numbers 1404465-1404467 for compounds **1** – **3**. See DOI: 10.1039/xxxxx for crystalographic data in CIF format.

Table 1. Crystallographic data and structure refinement results for compounds **1** - **3**.

Compound	**1**[a]	**2**[a]	**3**
Formula	$C_{30}H_{48}N_6O_{15}Cu$	$C_{114}H_{144}N_{20}O_{79}Cu_9$	$C_{62}H_{40}N_{10}O_{26}Cu_4$
Formula weight	796.29	3630.35	1595.20
Crystal system	Rhombohedral	Orthorhombic	Monoclinic
Space group	*R*-3	*P*nna	C2/c
a, Å	45.646(7)	32.4700(10)	16.6013(6)
b, Å	45.646(7)	22.1150(10)	13.2647(4)
c, Å	10.915(2)	20.2730(10)	29.6078(8)
α, °	90	90	90
β, °	120	90	92.656(3)
γ, °	90	90	90
V, Å^3	19695(6)	14557.5(11)	6513.0(4)
Z	18	4	4
Crystal Size, mm	0.23×0.25×0.33	0.17×0.22×0.26	0.12×0.14×0.20
D_c, g cm^{-3}	1.208	1.656	1.627
μ, mm^{-1}	0.563	1.401	2.279
Reflections collected	22302	191854	12402
Unique reflections	7632	16962	6067
R_{int}	0.0328	0.1090	0.0227
GOF	1.088	1.194	1.024
*R*1 [$I > 2\sigma(I)$]	0.0677	0.0663	0.0745
*wR*2 (all data)	0.2016	0.1827	0.2107
$\Delta\rho_{max}$, $\Delta\rho_{min}$, e Å^{-3}	1.086, -0.914	1.928, -1.027	2.231, -0.985

[a]The values in parenthesis are for the refinement after the SQUEEZE routine.

Results and discussion

Syntheses.

Crystals of compounds **1** - **3** were synthesized by hydrothermal reactions with good reproducibility. The products have been fully characterized by single-crystal X-ray diffraction, IR, EA, PXRD, and TGA techniques (see Fig. S1 and S2).

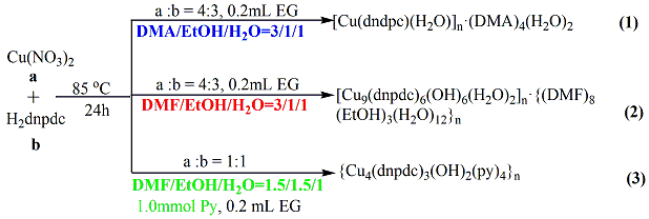

Scheme 1. The synthetic route of compounds **1**-**3**.

Solvothermal synthesis is a relatively complex process, and subtle changes of the synthesis conditions, such as temperature, reaction time, and the solvent, may impose a strong influence on the final structures. In our system, all the three compounds were prepared by reaction of the H_2dnpdc ligands and $Cu(NO_3)_2$ under solvothermal conditions in different mixed solvents (Scheme 1). Solvothermal synthesis (85°C) in the presence of 0.2mL of ethyl glycol (EG) in DMA-EtOH-H_2O (5mL, v/v/v=3/1/1) produces compound **1**, while the reaction in mixture of DMF-EtOH-H_2O results in compound **2**. Similarly, using a mixture of DMF-EtOH-H_2O-py as solvent, we isolated crystals of **3**. It is worthy to note that a little amount of ethyl glycol was used in the synthesis of **1**-**3**, to improve the quality and yield. In order to confirm the phrase purity of compounds **1**-**3**, the PXRD were performed with the bulk samples. As shown in Fig. S1 (see Supporting Information), the experimental PXRD patterns of complexes **1**-**3** are in good agreement with their corresponding simulated ones, confirming the purity of the as-synthesized samples. Although there are large cavities in compound **1** and **2** (approximately 67.8% and 46.1% of the crystal volume, respectively), we can not get the activated structures, because of the collapse of the structures after the guest molecules are being removed, which are similar some reported Cu-based MOFs with large porosity.

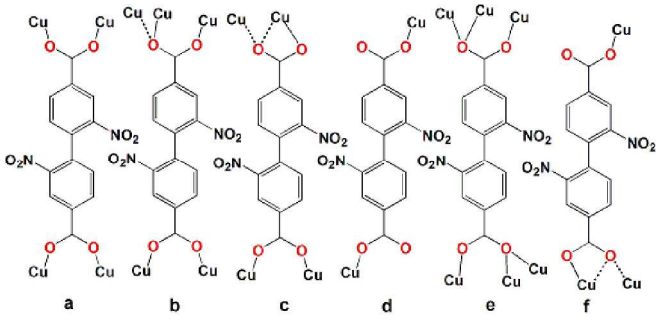

Scheme 2. Versatile coordination modes of H_2dnpdc observed in compounds **1**-**3** (the dotted lines represent weakly coordination to Cu^{II} centers with Cu-O distances being larger than 2.5 Å).

Crystal Structures

$[Cu(dnpdc)(H_2O)]_n\cdot(DMA)_4(H_2O)_2$ (1).

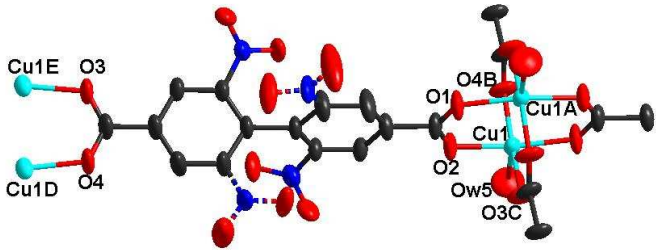

Fig. 1. ORTEP drawing of **1** with atomic numbering scheme (thermal ellipsoids at 30% probability), the dotted lines represent the disordered nitro groups (all hydrogen atoms and free guests are omitted for clarity).

Single-crystal X-ray diffraction revealed that compound **1** crystallizes in hexagonal space group *R*-3 and exhibits 2-fold interpenetrated 3D frameworks based on binuclear $[Cu_2(O_2C)_4]$

"paddle-wheel" SBU. The asymmetric unit consists of one Cu^{II} ion, a coordinated H_2O solvent, and one dnpdc^{2-} ligand. The Cu^{II} is coordinated in a square-pyramidal geometry (SP) with four carboxylate oxygen atoms from four dnpdc^{2-} ligands on the four corners and a water molecule at the top (Fig. 1). As expected, two symmetry equivalent Cu^{II} centers are bridged by four carboxylate groups from four different dnpdc^{2-} ligands, forming the well-known $[Cu_2(O_2C)_4]$ paddle-wheel SBU with the Cu…Cu distance of 2.669(2) Å. The average Cu-O_c (O_c represent the carboxylate oxygens) distance is 1.948 Å, and the Cu-O_w (O_w represent the water molecule) has a longer distance of 2.115(3) Å (Table S1), which is similar to those found in related $[Cu_2(O_2C)_4]$ paddle-wheel MOFs[15]. The dnpdc^{2-} ligand adopts the μ_4,η^4 coordination mode (Scheme 2a) to link four Cu^{II} ions using four carboxylate oxygen atoms. As founded in other compounds based on dnpdc ligands, the ligand adopts a highly twisted conformation with a dihedral angle of 74.97(11)° between the two phenyl rings, due to the steric hindrance of the two nitro groups in 2,2'-positions. Each $[Cu_2(O_2C)_4]$ paddle-wheel is linked with four neighbouring units through the dinitrobiphenyl backbones of dnpdc ligands to generate a 3D framework. Considering the $[Cu_2(O_2C)_4]$ paddle-wheel as four-connected nodes and the dintrobiphenyl group as linker, the structure has a *NbO* network of $6^4{\cdot}8^2$topology[15]. There are 1D hexagonal channels along the *c* axis with nitro groups decorated on the walls. In order to minimize the presence of large cavities and to stabilize the framework during the assembly process, other identical networks are filled in the cavities giving a 2-fold interpenetrating 3D architecture. Despite the 2-fold interpenetration, there is still large effective void volumes (67.8% calculated by *PLATON* program) in which the heavily disordered DMA and water molecules are filled, according to EA and TGA data[23]. Unfortunately, the attempts to remove the guest molecules giving activated compound **1** failed and resulted in collapse of the structure.

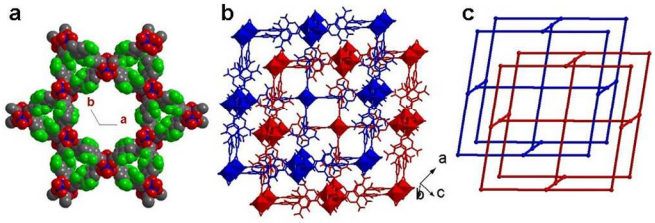

Fig. 2 (a) View of a single framework along the *c* direction showing hexagonal channels (the nitro groups are presented in green colour); (b) the 2-fold interpenetrated frameworks; (c) the 2-fold interpenetrated *NbO* nets.

$[Cu_9(dnpdc)_6(OH)_6(H_2O)_2]_n{\cdot}\{(DMF)_8(EtOH)_3(H_2O)_{12}\}_n$ (2)

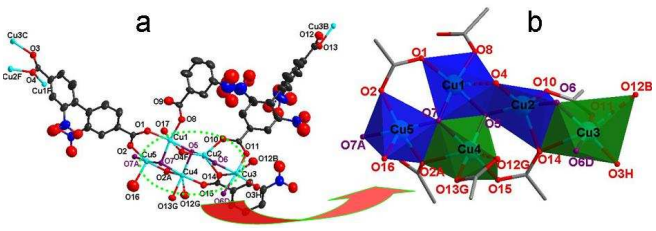

Fig. 3. (a) ORTEP drawing of **2** with atomic numbering scheme (thermal ellipsoids at 30% probability); (b) A close-up view of the pentanuclear motif.

When mixed solvent DMA-EtOH-H_2O for the syntheses of **1** is replaced with DMF-EtOH-H_2O, pale-green crystals of compound **2** with good yield are obtained, which exhibits 3D frameworks based on complicated 1D $[Cu(OH)(OCO)]_n$ chain. Single crystal X-ray diffraction revealed that compound **2** crystallizes in the orthorhombic *Pnna* space group and the asymmetric unit consists of five crystallographically independent Cu^{II} ions, three dnpdc ligands, three hydroxo anions, and two terminal H_2O molecules. As shown in Fig. 3, three Cu^{II} ions (Cu1, Cu3 and Cu4) are six-coordinated and adopt axially elongated octahedral geometry with somewhat difference. The equatorial plane is defined by two carboxylate oxygen atoms (O1 and O8 for Cu1, O3H and O11 for Cu3, O13G and O15 for Cu4) and two hydroxo anions (O5 and O7 for Cu1, O6 and O6D for Cu3, and O5 and O7 for Cu4, respectively). The weak coordinative oxygen atoms from terminal H_2O molecule and carboxylate groups (O17 and O4F for Cu1, O12B and O14 for Cu3; O2A and O12G for Cu4) occupy the axial positions with significantly longer Cu-O bond distances [2.426(3) Å - 2.710(4) Å] than the equatorial ones [1.905(3) Å - 1.975(2) Å]. For Cu4, due to the very small bite angle of the asymmetric carboxylato group (O12-Cu-O13, 55.20°), the equatorial base is significantly inclined relatively to the one of Cu3, leading to the highly distorted octahedron. Both Cu2 and Cu5 assume five-coordinated geometry. For Cu5, residing on a crystallographic 2-fold axis, the geometry is SP with a little distortion towards trigonal bipyramidal (TBP) as indicated by the very small distortion parameter τ = 0.14 (τ = 0 for ideal SP and 1 for ideal TBP)[24]. The basal donors include two carboxylate oxygen atoms (O2 and O2A) and two hydroxo anions (O7 and O7A) and the apex is furnished by a terminal coordination H_2O molecule (O16) with the apical bond length [2.222(7) Å] being obviously longer than the basal ones [1.912(3) Å - 2.007(2) Å]. Cu2 may also be said to be in SP geometry, but the distortion towards TBP is significant (τ = 0.48). The short basal bonds [1.918(3) Å - 2.007(3) Å] involve two carboxylate oxygen atoms (O4F and O10), two hydroxo anion (O5 and O6), and the long apical bond [2.155(3) Å] is formed by a third carboxylate oxygen (O14).

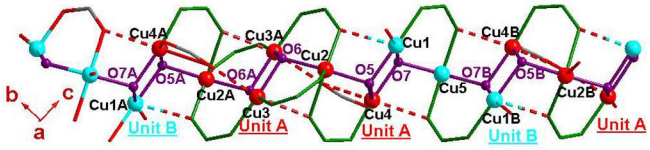

Fig. 4. The 1D chain in **2** with mixed hydroxo and carboxylate bridges.

The μ_3-hydroxo bridges collaborate with the carboxylate bridges to link the Cu^{II} ions into a complicated chain with an overall composition of $[Cu(OH)(OCO)]_n$. As shown in Fig. 4, the smallest repeating unit of the chain is a nine-nuclear motif, composed by three trinuclear units. Firstly, three trigonal-arranged Cu ions (Cu2, Cu3 and Cu4) are bridged by (μ_3-OH)(*syn*,*syn*-OCO) bridges into trinuclear unit (Unit A) and the Cu···Cu distances within the trinuclear motif are 3.095(1)

Å and 3.026(1) Å, and the corresponding Cu-O-Cu angles are 106.14(2)° and 101.53(1)°. Meanwhile, Cu1 and its equivalent Cu1B are bridged by central Cu5 through (μ_3-OH)(*syn*,*syn*-OCO) bridges, yielded the other trinuclear unit (Unit B) with the Cu···Cu distance and the corresponding Cu-O-Cu angle of 3.077(1) Å and 105.14(1)°, respectively. Secondly, two equivalent Unit A are linked by one Unit B through the four μ_3-hydroxo bridges (O5 and O7), forming the nine-nuclear motif with a slightly shorter Cu···Cu distance of 2.991(1) Å and smaller Cu-O-Cu angles of 98.66(2)° and 99.53(1)°, compared with the others described before. Lastly, the adjacent nine-nuclear units are further linked by μ_3-hydroxo groups into the complicated 1D $[Cu(OH)(OCO)]_n$, which are further stabled by the carboxylate groups.

In compound **2**, the fully deprotonated $dnpdc^{2-}$ ligand exhibits four different coordination modes (Scheme 2b-e), namely, $\mu_5\eta^4$ (two μ-1,3-carboxylates and meanwhile weakly coordinated to another Cu with one carboxylate oxygen atom), $\mu_4\eta^4$ (a μ-1,3-carboxylate and the other chelates and bridges two Cu ions), $\mu_2\eta^2$ (two monodentate carboxylate) and $\mu_6\eta^4$ (two μ-1,3-carboxylates and meanwhile weakly coordinated to another Cu with one carboxylate oxygen atom). The dihedral angle between the two phenyl rings for these four modes are 59.53(14)°, 83.91(21)°, 75.88(19)°, and 67.09(13)°, respectively. The $[Cu(OH)(OCO)]_n$ chains spanned along (011) and (01-1) directions, which are mostly penetrated to each other. Each $[Cu(OH)(COO)]_n$ chain is connected to four adjacent identical chains in different directions through the dinitrobiphenyl backbones of the dnpdc ligands, leading to the 3D framework with large cavities (Fig. S4). Calculation with *PLATON* software reveals that the effective void volume is about 6279.7 $Å^3$ per unit cell, comprising 43.1% of the crystal volume (14557.2 $Å^3$)[23], in which the solvent eight DMF, twelve H_2O and three ethanol molecules per formula are included, and thus the formula is $[Cu_9(dnpdc)_6(OH)_6(H_2O)_2]_n \cdot \{(DMF)_8(EtOH)_3(H_2O)_{12}\}_n$ according to crystallographic data combined with elemental and TG analyses.

$\{Cu_4(dnpdc)_3(OH)_2(py)_4\}_n$ (3)

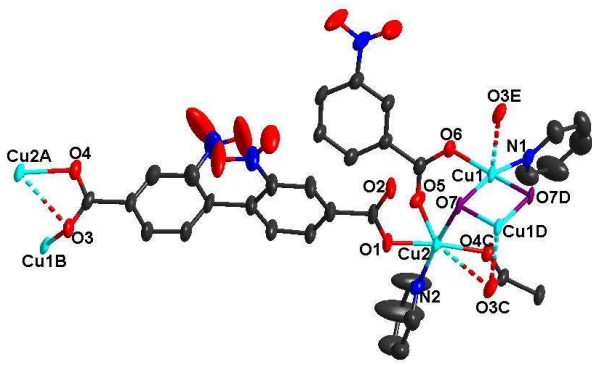

Fig. 5. ORTEP drawing of compound **3** with atomic numbering scheme (thermal ellipsoids at 30% probability).

When the reaction was done in DMF-Ethanol-H_2O mixture, using pyridine as template, we got compound **3**. Single-X-ray crystallographic analyses revealed that compound **3** crystallizes in the monoclinic C2/c space group and exhibits a 3D framework in which two μ_3-OH centred tetranuclear units are cross-linked by the dnpdc spacers. The asymmetric unit contains two Cu^{II} ions (Cu1 and Cu2), one and half dnpdc ligands, a μ_3-hydroxo anion and two terminal pyridine molecules. Selected bond distances and angles are listed in Table S2. Cu1 is four-coordinated [N1O3] in the distorted square-planar geometry, defined by one pyridyl nitrogen (N1), two hydroxo anions (O7 and O7D), and one carboxylate oxygen (O6). Cu2 is five-coordinated [N1O4] and resides in an axially elongated square pyramidal environment. The basal plane is defined by two carboxylate oxygens (O1 and O4C), a μ_3-hydroxo oxygen (O7) and a pyridyl nitrogen (N2), and a third carboxylate oxygen (O5) occupies the apical position. The apical bond distance [2.198(4) Å] is significantly longer than the basal ones [1.950(3)Å -2.000(3)Å]. The basal atoms are almost coplane, and Cu2 is out of the mean basal plane by 0.135(2) Å. The μ_3-OH bridge lies in the basal planes of all the Cu^{II} ions it binds. These features are of particular relevance to magnetic properties. It should be noted that Cu1D and Cu2 are bridged by O3C from the O3C-C14C-O4C carboxylate by weakly coordination interactions, with a rather long Cu-O distance of 2.535(4) Å and 2.679(4) Å, respectively. If this "weakly-coordination" is considered, the geometries around Cu1 and Cu2 may be described as elongated square pyramidal and highly distorted octahedron.

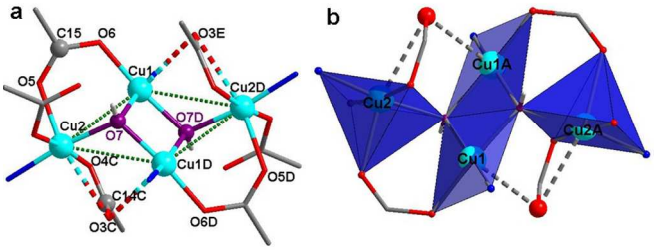

Fig. 6 (a) The tetranuclear $[Cu_4(\mu_3\text{-}OH)_2(OCO)_4]$ cluster in **3**; (b) The view showing the arrangement of the coordination polyhedra in the cluster.

As shown in Fig. 6, the tetracopper $[Cu_4(\mu_3\text{-}OH)_2(OCO)_4]$ cluster contains a centrosymmetric $[Cu_4(OH)_2]^{6+}$ core, in which four Cu^{II} atoms are linked by two equivalent μ_3-OH bridges (O7 and O7D) to form a planar rhombus. The geometry can also be described as two Cu_3O triagonal pyramids sharing the basal edge defined by two centrosymmetry-related and double hydroxo-bridged Cu1 atoms, with Cu1···Cu1A = 2.959(2) Å. The Cu-O-Cu angles around the μ_3-OH (O7) range from 98.5° to 112.4°. The sum (317°) of the three angles around μ_3-OH deviates much from 360°, and the μ_3-OH atom is displaced out of the Cu_3 plane by 0.76 Å, defining a rather flat pyramidal shape for Cu_3O. The tetranuclear $[Cu_4(\mu_3\text{-}OH)_2]^{6+}$ core is further reinforced by four carboxylate bridges. There are two different bridging fashions between Cu1 and Cu2 sites. One is the double bridging motif containing a μ_3-hydroxo and a μ_2-carboxylate in *syn-syn* coordination mode (O5-C15-O6), with Cu1···Cu2 = 3.145(1) Å; the other is the triple bridging motif containing a μ_3-hydroxo bridge, a μ_2-carboxylate in *syn-anti* coordination mode and a weakly coordinated μ_2-O bridge from the former carboxylate group, with larger Cu1A···Cu2 distance of

3.271(2) Å.

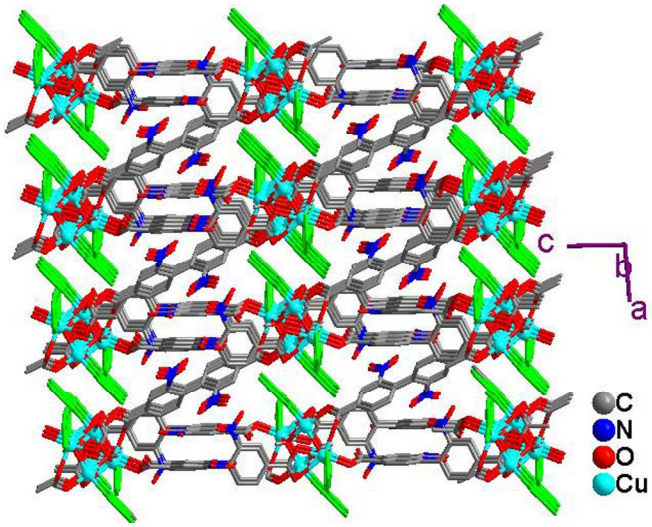

Fig. 7. The perspective view of the 3D framework in compound **3**, and the pyridyl molecules are highlighted in green colors.

The dnpdc ligands exhibit two different coordination mode (Scheme 2a and 2f): μ_4,η^4 (bis(μ-1,3-bridging) carboxylate), μ_3,η^3 (a monodentate carboxylate binding Cu2 and a μ-1,3-carboxylate binding two Cu1 and Cu2). The dihedral angle between the two phenyl rings for two modes are 71.28(17)º and 79.16(25)º, respectively. Each tetranuclear $[Cu_4(\mu_3\text{-}OH)_2]^{6+}$ cluster is linked to six neighbouring tetranuclear clusters through six $dnpdc^{2-}$ ligands, resulting in a 3D network (Fig. 7). Topologically, the tetranuclear cluster can be regarded as a 6-connected node, while the $dnpdc^{2-}$ ligand serves as a linker, the 3D structure of **3** can be reduced in to a 6-connected *pcu* net (Fig. 8).

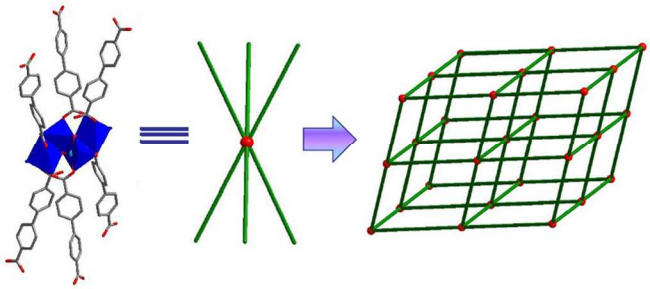

Fig. 8. View of the tetranuclear cluster serving as 6-connected node and the resulting *pcu* net (the nitro groups are omitted for clarity).

Magnetic properties

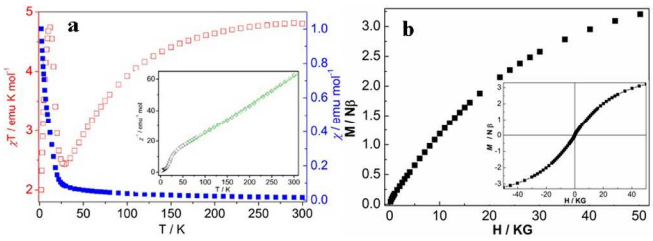

Fig. 9. The temperature dependence of $\chi_M T$ and χ_M^{-1} (inset) for **2**; (b) The field-dependent isothermal magnetization curve at 2K for **2** (inset: the whole field dependence of the magnetization emphasizing the absence of a hysteresis loop).

The magnetic susceptibilities (χ_M) of compound **2** and **3** have been carried out on crystalline samples under 1 kOe in the range of 2-300 K. For compound **2**, $\chi_M T$–T and χ_M^{-1}–T plots are shown in Fig. 9 (χ_M is the molar magnetic susceptibility of nine Cu^{II} ions). The $\chi_M T$ value at 300K is about 4.81 emu K mol^{-1}, which is evidently larger than the value 3.375 emu K mol^{-1} expected for nine magnetically isolated high-spin Cu^{II} ions with g = 2.0. As the temperature decreases, the $\chi_M T$ value reduces gradually to a minimum value of 2.44 emu K mol^{-1} at 28 K, then rises rapidly to a maximum value of 4.74 emu K mol^{-1} at 12 K, and finally drops rapidly to 2.00 emu K mol^{-1} at 2 K, and the rapid decrease of $\chi_M T$ value below 12 K may be best attributed to the saturation effect. The χ_M^{-1}–T plot above 40K follow the Curie-Weiss law with C = 5.47cm^3 mol^{-1} K, and θ = - 37.58 K. The high-temperature behaviour of $\chi_M T$ *versus* T and the negative θ value suggest that dominant antiferromagnetic interactions between the adjacent Cu^{II} centers are operative in compound **2**. The presence of low-temperature minima in the $\chi_M T$-T plot is characteristic of a ferrimagnetic system[25]. The ferrimagnetism may be arise from uncompensated moment of ferro-antiferromagnetic coupling within the chain, which can be explained in terms of topological ferrimagnetism induced by irregular alternate pair of antiferromagnetic interactions and at least one ferromagnetic coupling, considering the homospin character of the compound.

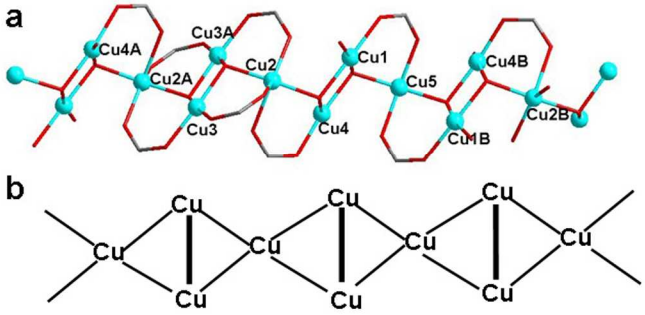

Fig. 10. (a) View of the 1D spin chain; (b) the ferrimagnetic scheme of the chain in compound **2**.

Neglecting the interactions between the $[Cu(OH)(OCO)]_n$ chains, which are well separated by the long biphenyl spacers of the $dnpdc^{2-}$ ligands. As described in the structural part of compound **2**, there are three kinds of magnetic exchange pathways in compound **2**: $Cu(OH)_2Cu$, Cu(OH)(OCO)Cu and Cu(OH)Cu (Fig. 10). Cu3 with its equivalent Cu3A and Cu1 with Cu4 are both double μ_3-OH bridged with Cu-O-Cu angle of 100.84(2)°, 98.66(2)° and 99.53(2)°, respectively, which are all larger than 97.5°, so the antiferromagnetic coupling should be dominate[26]. Considering that Cu2 with Cu3, Cu2 with Cu4, and Cu1with Cu5 are all double bridged through μ_3-OH and *syn-syn*-OCO bridges and the negative J values of Cu(OH)(OCO)Cu and Cu $(OH)_2Cu$ of complex **3** mentioned below, we assigned the antiferromagnetic coupling to the mixed double μ_3-OH and *syn-syn*-OCO bridges and the double μ_3-OH bridges, and tentatively assigned the

ferromagnetic coupling to the single μ_3-OH bridge between Cu1 and Cu2. However, we cannot quantitatively evaluate the interactions through different bridges, for the lack of an appropriate model for such a compound system. The ferrimagnetic behaviour of **2** was further characterized by field dependent magnetization measurements at 2.0 K (Fig. 9b). As the applied field increases, the magnetization increases smoothly and reaches to a magnetization of ca. 3.21 Nβ at 50 kG, which is much lower than that expected for a total alignment of the moments. No magnetic hysteresis is observed at 2.0 K for compound **2**.

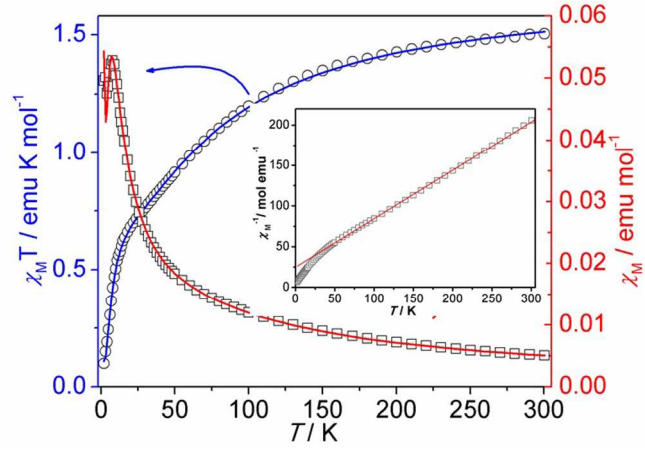

Fig. 11. The temperature dependence of $\chi_M T$, χ_M and χ_M^{-1} (inset) curves for **3**, the solid lines represent the best fit of the data to the model described in the text.

For compound **3**, The $\chi_M T$ value at room temperature is about 1.505 emu K mol^{-1}, comparable with the spin-only value (1.50 emu K mol^{-1} from g = 2.00) expected for four magnetically isolated Cu^{II} ions. Upon cooling, the $\chi_M T$ value decreases continuously, while the χ_M value increases smoothly to a sharp maximum value of 0.053 emu mol^{-1} at ca. 8 K and then decreases rapidly towards zero at lower temperature. The decrease of $\chi_M T$ with decreased temperature clearly indicates antiferromagnetic interactions in this compound. The χ_M^{-1}-T plot above 50 K follows the Curie-Weiss law with C = 1.68 emu K mol^{-1} and θ = -41.42 K. The negative θ value also confirms the overall antiferromagnetic coupling between the Cu^{II} ions, and the C value fall in the usual range of expected for Cu^{II}.

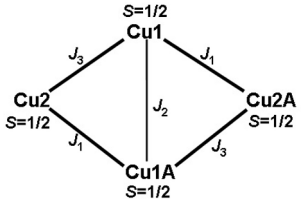

Scheme 3. Diagram showing the definition of atom number and magnetic exchange parameters of the tetracopper cluster in compound **3**.

As demonstrated in the structural discussion, compound **3** presents a 3D network, constructed from the [$Cu_4(\mu_3$-$OH)_2(OCO)_4$] tetracopper cluster. The magnetic interactions through the long dnpdc ligands should be negligible, so the compound may be treated as magnetically isolated Cu_4 cluster. Based on the structural data, there are three different sets of connection between Cu^{II} ions in the tetranuclear rhombic cluster: Cu1(OH)(OCO)Cu2, Cu2(OH)(O)(OCO)Cu1A, and Cu1$(OH)_2$Cu1A. The superexchange scheme can be represented as follows (Scheme 3), so the spin Hamiltonian is

$H = -2J_1(S_{2A}S_{1A} + S_2S_1) - 2J_2S_{2A}S_2 - 2J_3(S_{2A}S_1 + S_2S_{1A})$. The energy matrix can be solved to give the following six energy levels with the total spin S = 0, 1 and 2:[27]

$E_1 = -J_1 - J_2/2 - J_3$, $S = 2$.

$E_2 = J_1 - J_2/2 + J_3$, $S = 1$.

$E_3 = J_2/2 + [J_2^2 + (J_3 - J_1)^2)]^{1/2}$, $S = 1$.

$E_4 = J_2/2 - [J_2^2 + (J_3 - J_1)^2)]^{1/2}$, $S = 1$.

$E_5 = J_1 + J_3 + J_2/2 + [4(J_1^2 + J_3^2) + J_2^2 - 4J_1J_3 - 2J_2J_3 - 2J_1J_2]^{1/2}$, $S = 0$.

$E_6 = J_1 + J_3 + J_2/2 - [4(J_1^2 + J_3^2) + J_2^2 - 4J_1J_3 - 2J_2J_3 - 2J_1J_2]^{1/2}$, $S = 0$.

Applying the energy eigenvalues to the van Vleck equation yields the following molar magnetic susceptibility of the tetracopper cluster:

$$\chi = \frac{2N\beta^2 g^2}{kT}\left(\frac{A}{B}\right)$$

with $A = 5\exp(-E_1/kT) + \exp(-E_2/kT) + \exp(-E_3/kT) + \exp(-E_4/kT)$, and $B = 5\exp(-E_1/kT) + 3\exp(-E_2/kT) + 3\exp(-E_3/kT) + 3\exp(-E_4/kT) + \exp(-E_5/kT) + \exp(-E_6/kT)$.

Fitting the experimental data for **3** by the above expression led to J_1 = -17.0 cm^{-1}, J_2 = -32.4 cm^{-1}, J_3 = -19.6 cm^{-1} and g = 2.10. The J_2 values suggest a moderate antiferromagnetic interaction through the double hydroxo bridges between Cu1 and Cu1A. A lot of studies have revealed the interaction in the double hydroxo bridged Cu^{II} systems is sensitive to the Cu-O-Cu angles and the crossover angle is ca. 97.5°, above which the antiferromagnetic interaction increases with the angles[26, 27]. In compound **3**, the Cu1-O-Cu1A angle (98.5(1)°) is larger than 97.5°, and hence exhibits a antiferromagnetic interaction. The J_1 and J_3 values suggest the interactions through the mixed triple [(OH)(O)(OCO)] and double [(OH)(OCO)] bridges are also antiferromagnetic. As has been noted, the carboxylate oxygen atom (O3) is weakly coordinated to Cu1A and Cu2 with Cu-O bond length both being larger than 2.5Å [2.679(4) Å and 2.535(4) Å, respective], such bridge is not expected to be a good pathway for superexchange. The magnetic exchange through the (O)(OCO) bridge between Cu1A and Cu2 can be neglected. On the other hand, as we all know, since the magnetic orbital of Cu^{II} in axially elongated square-pyramidal geometry is of the d_{x2-y2} type with no significant delocalization towards axial ligands, the magnetic coupling through the apical-equatorial bridge should be negligibly small[28], so an eq–ax carboxylate bridge between Cu1 and Cu2 can also be neglected from magnetic viewpoint. Thus, both double and triple motifs have only a hydroxo as effective exchange pathway. However, the incorporation of weakly coordinated carboxylate oxygen atom and eq-ax carboxylate group may be responsible for the increased Cu-O-Cu angle and Cu...Cu distance in the triple motif compared with the double motif, and hence may influence magnetic coupling in an indirect

way. The smaller J_1 parameters may be assigned to the double motif, which has a smaller Cu–O–Cu angle, but the assignment should be regarded as being very tentative because the J_1 and J_3 values are very close to each other in **3**.

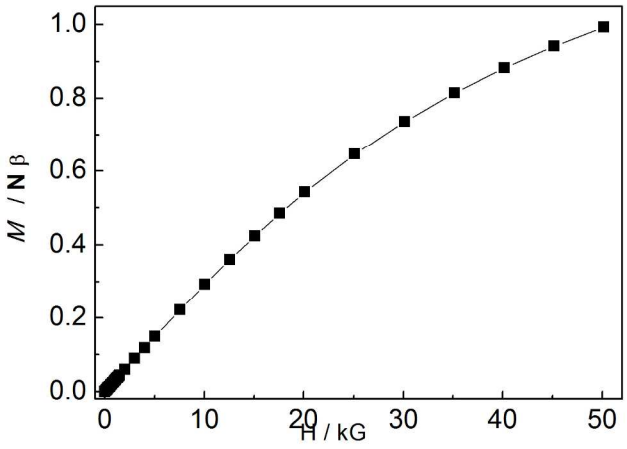

Fig. 12. The field-dependent isothermal magnetization curve for compound **3** at 2K.

The isothermal magnetization curve for **3** was measured from 0 to 50 kG at 2 K (Fig. 12). The magnetization curve is quasi-linear, and the value at 50 kG ($0.99N\beta$) is far from the saturation value excepted for four non-coupled Cu^{II} ions.system ($>4N\beta$ considering that g_{Cu} is usually larger than 2.0). This is characteristic of an antiferromagnetic system, which is consistent with the antiferromagnetic interactions between the Cu^{II} ions in compound **3**.

Conclusions

In summary, we have described the hydrothermal synthesis, structures and magnetic properties of three Cu-based on MOFs derived from 2,2′-dinitrobiphenyl-4,4′-dicarboxylic acid (H_2dnpdc) and Cu^{II} ions. The resulting structures of the MOFs are highly dependence on the solvent used during the synthesis. Compound **1**, exhibits 2-fold interpenetrated 3D coordination network based on binuclear $[Cu_2(O_2C)_4]$ "paddle-wheel" SBU. In compound **2**, the Cu^{II} ions are connected by a mixture of μ_3-OH, and μ-COO bridges to give complicated 1D chain spanned in two directions, which are cross-linked into a 3D framework by $dnpdc^{2-}$ ligands. Compound **3** exhibits 3D frameworks in which tetranuclear $[Cu_4(\mu_3\text{-}OH)_2(OCO)_4]$ cluster are linked by the dnpdc spacers. Magnetic studies reveal compound **2** exhibits homospin topological ferrimagnetism and the μ_3-OH and carboxylate mixed bridges mediate antiferromagnetic interactions between the Cu^{II} ions in compound **3**.

Acknowledgement

We are thanking for the financial support of NSFC (21173083 and 91022017), the Foundation of Science and Technology Development of Shanghai (14ZR1447900), Key Discipline Grant for Composite Materials from Shanghai Institute of Technology (No. 10210Q140001) and the Fundamental Research Funds for the Central Universities.

References

[a] *Shanghai Institute of Technology, Shanghai 200235, China. E-mail: jianyong1106@163.com.*
[b] *Department of Chemistry, School of Science, Xi'an Jiaotong University, Xi'an 710049, China.*
[c] *Shanghai Key Laboratory of Green Chemistry and Chemical Processes, Department of Chemistry, East China Normal University, Shanghai 200062, China. E-mail: eqgao@chem.ecnu.edu.cn.*

1 (a) S. R. Batten, S. M. Neville, D. R. Turner, *Coordination Polymers Design, Analysis and Application*; The Royal Society of Chemistry: London, 2009; pp 273; (b) S. Kitagawa, K. Uemura, *Chem. Soc. Rev.,* 2005, **34**, 109; (c) D. Zhao, D. J. Timmons, D. Q. Yuan, and H.-C. Zhou, *Acc. Chem. Res.,* 2011, **44**, 123; (d) L. Chen, Q. Chen, M. Wu, F. Jiang, and M. Hong, *Acc. Chem. Res*., 2015, **48**, 201.

2 (a) J.-R. Li, Y. Ma, M. C. McCarthy, J. Sculley, J. Yu, H.-K. Jeong, P. B. Balbuena, H.-C. Zhou, *Coord. Chem. Rev*., 2011, **255**, 1791; (b) M. P. Suh, H. J. Park, T. K. Prasad, D.-W. Lim, *Chem. Rev*., 2012, **112**, 782; (c) D. Farrusseng, (Ed.), Metal-Organic Frameworks: Applications from Catalysis to Gas Storage, Wiley-VCH, Weinheim, 2011.

3 (a) L. Ma, C. Abney, and W. Lin, *Chem. Soc. Rev.,* 2009, **38**, 1248; (b) J. Y. Lee, O. K. Farha, J. Roberts, K. A. Scheidt, S. B. T. Nguyen, and J. T. Hupp, *Chem. Soc. Rev.,* 2009, **38**, 1450; (c) M. Yoon, R. Srirambalaji, K. Kim, *Chem. Rev.*, 2012, **112**, 1196.

4 (a) P. Horcajada, C. Serre, M. Vallet-Regi, M. Sebban, F. Taulelle, and G. Férey, *Angew. Chem., Int. Ed.,* 2006, **45**, 5974; (b) W. J. Rieter, K. M. Pott, K. M. L.Taylor, W.-B.Lin, *J. Am. Chem. Soc.,* 2008, **130**, 11584.

5 (a) Y. J. Cui, Y. F. Yue, G.-D. Qian, and B.-L. Chen, *Chem. Rev*., 2012, **112**, 1126; (b) M.-J. Dong, M. Zhao, S. Ou, C. Zou, C.-D. Wu, *Angew. Chem., Int. Ed.,* 2014, **53**, 1575.

6 (*a*) L. E. Kreno, K. Leong, O. K. Farha, M. Allendorf, R. P. V. Duyne, and J. T. Hupp, *Chem. Rev*., 2012, **112**, 1105; (b) X, Lin, G. Gao, L. Zheng, Y. Chi, G. Chen, *Anal. Chem*., 2014, **86**, 1223; (c) Y. Lu, and B. Yan, *Chem. Commun*., 2014, **50**, 13323.

7 (a) X.-Y. Wang, L. Wang, Z.-M. Wang, and S. Gao, *J. Am. Chem. Soc*., 2006, **128**, 674; (b) J. Ribas, A. Escuer, M. Monfort, R. Vicente, R. Cortés, L. Lezama, and T. Rojo, *Coord. Chem. Rev*., 1999, **193**, 1027; (c) J. Ribas, A. Escuer, M. Monfort, R. Vicente, R. Cortés, L. Lezama, and T. Rojo, *Coord. Chem. Rev*., 1999, **193**, 1027; (d) M. Kurmoo, *Chem. Soc. Rev.,* 2009, **38**, 1353 and references therein.

8 (a) L.-S. Long, *CrystEngComm*, 2010, **12**, 1354; (b) K. P. Rao, M. Higuchi, J. Duan, and S. Kitagawa, *Cryst. Growth Des*., 2013, **13**, 981; (c) Y.-X. Tan, Y.-P. He, Y. Zhang, Y.-J. Zheng, and J. Zhang, *CrystEngComm*, 2013, **15**, 6009.

9 (a) N. Zhang, Y.-J. Sun, H. Yang, J.-Y. Zhang, E.-Q. Gao, *Inorg. Chim. Acta*, 2015, **428**, 37; (b) J.-Y. Zhang, Y. Ma, A.-L. Cheng, Q. Yue, Q. Sun, and E.-Q. Gao, *Dalton Trans*., 2011, **40**, 7219; (c) J.-Y. Zhang, X.-H. Jing, Y. Ma, A.-L. Cheng and E.-Q. Gao, *Cryst. Growth Des*., 2011, **11**, 3681; (d) X.-H. Jing, X.-C. Yi, E.-Q. Gao, and V. A. Blatov, *Dalton Trans*., 2012, **41**, 14316.

10 (a) X. Zhao, L. Zhang, H. Ma, D. Sun, D. Wang, S. Feng, and D. Sun, *RSC Adv*., 2012, **2**, 5543; (b) B. Zhang, J. Zhang, C. Liu, X. Sang, L. Peng, X. Ma, T. Wu, B. Han, and G. Yang, *RSC Adv*., 2015, **5**, 37691; (c) C. P. Li, M. Du, *Chem. Commun*., 2011, **47**, 5958; (d) D. Frahm, F. Hoffmann, M. Fröba, *Cryst. Growth Des*., 2014, **14**, 1719.

11 (a) M.-H. Zeng, W.-X. Zhang, X.-Z. Sun, and X.-M. Chen, *Angew. Chem. Int. Ed.,* 2005, **44**, 3079; (b) G. J. Halder, C. J. Kepert, B. Moubaraki, K. S. Murray and J. D. Cashion, *Science*, 2002, **298**, 1762; (c) G.-C. Xu, W. Zhang, X.-M. Ma, Y.-H. Chen, L. Zhang, H.-L. Cai, Z.-M. Wang, R.-G. Xiong, and S. Gao, *J. Am. Chem. Soc*., 2011, **133**, 14948; (d) Q. Li, C. Tian, H. Zhang, J. Qian and S. Du, *CrystEngComm*, 2014, **16**, 9208; (e) D.-M. Chen, X.-Z. Ma, X.-J. Zhang, N. Xu, and P. Cheng, *Inorg. Chem.,* 2015, 5**4**, 2976;.

12 (a) Y. Ma, N. A. G. Bandeira, V. Robert, and E.-Q. Gao, *Chem. Eur. J.,* 2011, **17**, 1988; (b) W.-W. Sun, C.-Y. Tian, X.-H. Jing, Y.-Q. Wang, and E.-Q. Gao, *Chem. Commun*., 2009, 4741; (c) Y.-Q. Wang, Q.-X. Jia, K. Wang, A.-L. Cheng and E.-Q. Gao, *Inorg. Chem*., 2010, **49**, 1551; (d) E.-Q. Gao, Y.-F. Yue, S.-Q. Bai, Z. He, and C.-H. Yan, *J. Am. Chem. Soc*., 2004, **126**, 1419.

13 (a) Z.-M. Wang, B. Zhang, M. Kurmoo, M. A. Green, H. Fujiwara, T. Otsuka, H. Kobayashi, *Inorg. Chem*., 2005, **44**, 1230; (b) M. Du, X.-H. Bu, Y.-M. Guo, L. Zhang, D.-Z. Liao, J. Ribas, *Chem. Commun*., 2002, 1478; (c) G. B. Deacon, R. J. Phillips, *Coord. Chem. Rev*.,1980, **33**, 227.

14 (a) X. Zhu, J.-W. Zhao, B.-L. Li, Y. Song, Y.-M. Zhang, and Y. Zhang, *Inorg. Chem*., 2010, **49**, 1266; (b) X.-M. Zhang, Y.-Q. Wang, and E.-Q. Gao, *Eur. J. Inorg. Chem*., 2010, 1249; (c) S. Meenakumari, A. R. Chakravarty, *J. Chem. Soc., Dalton Trans*., 1992, 2305; (d) J. A. Sheikh, H. S. Jena, A. Adhikary, S. Khatua, S. Konar, *Inorg. Chem*., 2013, **52**, 9717.

15 (a) S. S.-Y. Chui, S. M.-F. Lo, J. P. H. Charmant, A. G. Orpen, I. D. Williams, *Science*, 1999, **283**, 1148; (b) A. Pichon, C. M. Fierro, M. Nieuwenhuyzen, and S. James, *CrystEngComm*, 2007, **9**, 449; (c) H. Furukawa, J. Kim, N. W. Ockwig, M. O'Keeffe, and O. M. Yaghi, *J. Am. Chem. Soc*., 2008, **130**, 11650.

16 (a) M. S. E. Fallah, A. Escuer, R. Vicente, F. Badyine, X. Solans, M. Font-Bardia, *Inorg. Chem.,* 2004, **43**, 7218; (b) J.-Y. Zhang, X.-B. Li, K. Wang, Ma, Y. A.-L. Cheng, E.-Q. Gao, *Dalton Trans*., 2012, **41**, 12192.

17 (a) J.-P. Zhao, B.-W. Hu, Q. Yang, T.-L. Hu, X.-H. Bu, *Inorg. Chem.* 2009, **48**, 7111; (b) C. López, R. Costa, F. Illas, C. de. Graaf, M. M.Turnbull, C. P. Landee, E. Espinosa, I. Mata, E. Molins, *Dalton Trans.,* 2005, 2322.

18 (a) Z. He, Z.-M. Wang, S. Gao, C.-H. Yan, *Inorg. Chem.,* 2006, **45**, 6694; (b) Y. Ma, A.-L. Cheng, B. Tang, E.-Q. Gao, *Dalton Trans.* 2014, **43**,13957; (c) Y.-F. Zeng, J.-P. Zhao, B.-W. Hu, X. Hu, F.-C. Liu, J. Ribas, J. Ribas-Ari, X.-H. Bu, *Chem. Eur. J.,* 2007, **13**, 9924.

19 (a) H. Tian, Q.-X. Jia, E.-Q. Gao, and Q.-L. Wang, *Chem. Commun*., 2010, **46**, 5349; (b) Q.-X. Jia, Y.-Q. Wang, Q. Yue, Q.-L. Wang, and E.-Q. Gao, *Chem. Commun*., 2008, 4894; (c) P.-P Liu,. A.-L. Cheng, N. Liu, W.-W. Sun, and E. -Q.Gao, *Chem. Mater*., 2007, **19**, 2724; (d) Q. Sun, A.-L. Cheng, Y.-Q. Wang, Y. Ma, and E.-Q. Gao, *Inorg. Chem*., 2011, **50**, 8144.

20 A. T. Nielsen, A. A. Defusco, and T. E. Browne, *J. Org. Chem.,* 1985, **50**, 4211.

21 Sheldrick, G. M. Program for Empirical Absorption Correction of Area Detector Data; University of Göttingen, Germany, 1996.

22 (a) G. M. Sheldrick, *SHELXTL* Version 5.1. Bruker Analytical X-ray Instruments Inc., Madison, Wisconsin, USA, 1998; (b) G. M. Sheldrick, *SHELXL-97*, PC Version. University of Göttingen, Germany, 1997.

23 A. L. Spek, *PLATON*, a multipurpose crystallographic tool; Utrecht University: Utrecht, The Netherlands, 2001.

24 W. Addison, T. N. Rao, J. Reedijk, J. Van Rijn, and G. C. Verschoor, *J. Chem. Soc., Dalton Trans*., 1984, 1349.

25 (a) H. O. Stumpf, Y. Pei, L. Ouabab, F. L. Berre, E. Codjovi, and O. Kahn, *Inorg. Chem.* 1993, **32**, 5678; (b) Z. Chen, L. Liu, Y. Wang, H. Zou, Z. Zhang, and F. Liang, *Dalton Trans*., 2014, **43**, 8154.

26 C. López, R. Costa, F. Illas, C. de Graaf, M. M. Turnbull, C. P. Landee, E. Espinosa, I. Mata, and E. Molins, *Dalton Trans*., 2005, 2322.

27 (a) R. W. Jotham, S. F. A. Kettle, *Inorg. Chim. Acta* 1970, **4**, 145; (b) Y.-F. Song, C. Massera, O. Roubeau, P. Gamez, A. M. M. Lanfredi, J. Reedijk, *Inorg. Chem.,* 2004, **43**, 6842.

28 (a) S. Triki, J. C. Gómez-García, E. Ruiz, J. Sala-Pala, *Inorg. Chem.* 2005, **44**, 5501; (b) S.-Q. Bai, E.-Q. Gao, Z. He, C.-J. Fang, C.-H. Yan, *New J.Chem.* 2005, **29**, 935.

29 (a) R. D. Willett, and G. L. Breneman, *Inorg. Chem*., 1983, **22**, 326; (b) L. Deakin, A. M. Arif, and J. S. Miller, *Inorg. Chem*., 1999, **38**, 5072; (c) P. Talukder, S. Sen, S. Mitra, L. Dahlenberg, C. Desplanches and J.-P. Sutter, *Eur. J. Inorg. Chem*., 2006, 329; (d) D. Ghoshal, T. K. Maji, G. Mostafa, S. Sain, T.-H. Lu, J. Ribas, E. Zangrando and N. R. Chaudhuri, *Dalton Trans*., 2004, 1687.